Oxidation of W(110) studied by LEED and STM

K. Radican, S.I. Bozhko, Sundar-Raja Vadapoo, S. Ulucan, Han-Chun Wu, A. McCoy, I.V. Shvets

PII: S0039-6028(10)00218-9
DOI: doi: 10.1016/j.susc.2010.05.016
Reference: SUSC 18994

To appear in: *Surface Science*

Received date: 5 March 2010
Accepted date: 11 May 2010

Please cite this article as: K. Radican, S.I. Bozhko, Sundar-Raja Vadapoo, S. Ulucan, Han-Chun Wu, A. McCoy, I.V. Shvets, Oxidation of W(110) studied by LEED and STM, *Surface Science* (2010), doi: 10.1016/j.susc.2010.05.016

Oxidation of W(110) studied by LEED and STM

K. Radican S.I. Bozhko Sundar-Raja Vadapoo S. Ulucan
Han-Chun Wu A. McCoy I.V. Shvets

CRANN, School of Physics, Trinity College Dublin, Dublin 2, Ireland

Abstract

The oxidation of W(110) was studied over a temperature a range of 1000 K to 1600 K at 1x10^{-6} Torr oxygen. The subsequent oxide structure was then characterized using Low Energy Electron Diffraction (LEED) and Scanning Tunneling Microscopy (STM). It was found that the resulting structure was remarkably similar to that of Mo(110)oxidized under similar conditions. Using the Mo(110) oxide structure as our basis, along with atomic resolution STM images, we have constructed a model for the surface oxide of W(110).

1 Introduction

Understanding the mechanisms of the initial growth stages of transition metal oxides is interesting for both the applied and fundamental sciences. These oxides often have unique electrical and chemical properties making them important in many areas of industry, including surface coatings, and for industrial catalysts. They are used in oxidation reactions for fuel processing, chemical production, and pollution cleanup.

Over the years there has been considerable attention given to the oxygen structures in the W(110) surface. The ordered phases of adsorbed oxygen up to one monolayer are well characterized [1–7]. From room temperature up to 700 K and low oxygen pressure there are three chemabsorbed structures, p(2x1) , p(2x2) and p(1x1), corresponding to $\frac{1}{2}$, $\frac{3}{4}$, and 1 monoyayer coverage respectively[3]. With temperatures above 700 K and O_2 pressures of ˜10^{-6} Torr an oxide structure with a complex LEED pattern is reported[8,2,9,5]. Earlier measurements concluded that the superstructure spots seen in LEED,

Email address: radicak(at)TCD.ie (I.V. Shvets).

which were described as c(14 x 7) in symmetry, were due to a compressed misfit overlayer [2]. This pattern, now more commonly referred to as a (1 x 1) x 12 has since been studied by a number of methods such as low energy electron diffraction (LEED), Auger electron spectroscopy (AES), thermal desorption spectroscopy, work function measurements, Photoelectron holography, X-ray photoelectron diffraction (XPD), and scanning tunneling microscopy (STM). The exact composition of this superstructure is still under debate. [2,5,6,8–11]. STM measurements made by Johnson et al. [10] found a local (1 x 1) symmetry of oxygen atoms that sit in the pseudo-threefold hollow sites of the (110) surface. This is the same site thought to be occupied in the p(2 x 1) structure formed at 0.5 monolayer (ML) [12]. Also, as part of the STM study [10], the superstructure spots in the LEED pattern were explained by two types of striped (1 x 1) domains related by a site-exchange of two equivalent threefold-hollow adsorption sites on the surface, spaced at regular intervals of about 33 Å giving a (1 x 12) periodicity along the [1 $\bar{1}$ 3] and [$\bar{1}$ 13] directions (cf. Fig. 1 of Ref. [10]). In a more recent LEED and X-ray photoelectron diffraction (XPD) study, Daimon et al. [9] again found this periodicity to be (1 x 12)but with striped domains align along the [1 $\bar{1}$ 2] and [11$\bar{2}$] directions, about 10° in azimuth away from the [1$\bar{1}$3] and [$\bar{1}$13] directions seen previously. However, it is still unclear as to why it chooses to have the (1 x 1) x 12 periodicity on our surface, or other periodicities in prior studies.

Recently, considerable steps have been made in the microscopic understanding of oxide formation on TM surfaces. By combining experimental data with density functional theory (DFT) calculations, researchers have been able to gain vast insight in the formation of these oxides [13–21]. These studies have lead to some rather complex models for the initial oxide formation. For late transition metals and noble metals such as Pd and Ag it is now known that the oxidation process proceeds through ultrathin oxide layers, that are thermodynamically stable [22–25]. The initial oxidation stages of Pd(111), Pd(100), Rh(111), Rh(110), Rh(100) and Mo(110) all show a common feature [18,20,23,25,26]. Their formation involves subsurface penetration of oxygen, likely through place exchange, resulting in the metal atoms being sandwiched between two atomic layers of oxygen, forming Oxygen-Metal-Oxygen (O-M-O) trylayer surface oxides. However, it was recently suggested that since many of the TM oxides wet their own metal surfaces, the adhesion energy should provide extra stabilization allowing a bulk-like surface oxide to form when the O_2 partial pressure is many orders of magnitude lower than required to maintain the bulk oxide [21]. In this paper we show that the initial oxidation stages of W(110) follow this trend, resulting in a bulk like WO_2 O-M-O try-layer surface oxide.

2 Material and methods

For this study we used single crystal W(110) with the surface deviation from the (110) plane of less than 0.1°. This substrate was placed in an ultra-high vacuum (UHV) chamber of base pressure below 10^{-10} Torr. The chamber is equipped with Low Energy Electron Diffraction (LEED) and a Createc low temperature Scanning Tunnelling Microscopy (LT-STM). The W substrates were first cleaned using a standard procedure based on annealing the substrate at 1900 K in an O_2 atmosphere of 1 x 10^{-7} Torr to remove surface carbon contamination, followed by a series of high-temperature (2200 K) flashes to remove the surface oxides. This process was repeated until a sharp W(110) p(1x1) LEED pattern was imaged. For these experiments the ultra pure oxygen was introduced to the chamber via a leak valve. The sample was heated via electron beam bombardment and temperatures were measured with an optical pyrometer (Ircon UX20P, emissivity 0.35).

All STM images were recorded at 77 K in constant current mode using currents of approximately 0.05 to 0.1 nA. The sample was biased with respect to the electrochemically etched W tips.

3 Results and discussion

Once a clean surface was obtained the samples were subject to a series of oxidations at a temperature range of 1000 K to 1600 K with 100 K increments. The chamber pressure was held constant at 1x10^{-6}Torr oxygen, and the annealing durations were 15, 60, 90 and 180 minutes. The resulting surfaces were then characterized using LEED and LT-STM.

3.1 LEED

After each oxidation a LEED pattern was taken, and in all cases the results were the same. This pattern, which is shown in figure 1, consists of the primary W(110) spots each with several orders of satellite spots visible. These satellite spots form rows along the [7 $\bar{7}$ $\bar{6}$] and [7 $\bar{7}$ 6] directions, 32°off [1 $\bar{1}$ 0], with a a spot spacing equal 9 spacings along [1 $\bar{1}$1] or 24.6 ± 1 Å in real space. This pattern can be explained as the result of two equivalent overlayer domains on the surface. However, for simplicity we will discuss things using only one domain. From LEED we can measure the orientation and dimensions of the oxide superstructure with respect to the W(110) surface, but get no details of it's atomic structure. This domain, illustrated by the yellow parallelogram on

Fig. 1. LEED image taken at 70 eV of W(110) oxidized with 1 x 10^{-6}Torr oxygen at 1600 K for 60min.

the (11) tungsten spot, can be defined in matrix notation as

$$\begin{bmatrix} 0 & 9 \\ -2 & 5 \end{bmatrix}$$

. In real space this gives a oxide overlayer unitcell of 24.6 Å along the W [1 $\bar{1}$ 1] direction and 13.0 Å along the W [$\bar{3}$ 3 7].

This LEED pattern is confusingly similar to that of the (1x1)x12 which has domains along the [$\bar{1}$ 1 3] or [$\bar{1}$ 1 2] as described in earlier studies[2,5,8,9]. For clarity, figure 2 shows LEED diagrams of each case with A, B, C, representing the [$\bar{1}$ 1 3], [$\bar{1}$ 1 2], and the [$\bar{3}$ 3 7] respectively. It can be seen that for the [$\bar{1}$ 1 3] and [$\bar{1}$ 1 2] cases the angle between the rows of spots and [1 $\bar{1}$ 0] is 25°and 35°respectively, i.e. there is a 10°angle between these two cases, and the [$\bar{1}$ 3 7] case lies in between the two at 31°from [1 $\bar{1}$ 0]. It is unclear why there is such a variety of similar structures that appear in this surface under similar preparation conditions. These discrepancies my arise due to slight changes in sample preparation such as post annealing, or from differing interpretations of the experimental data.

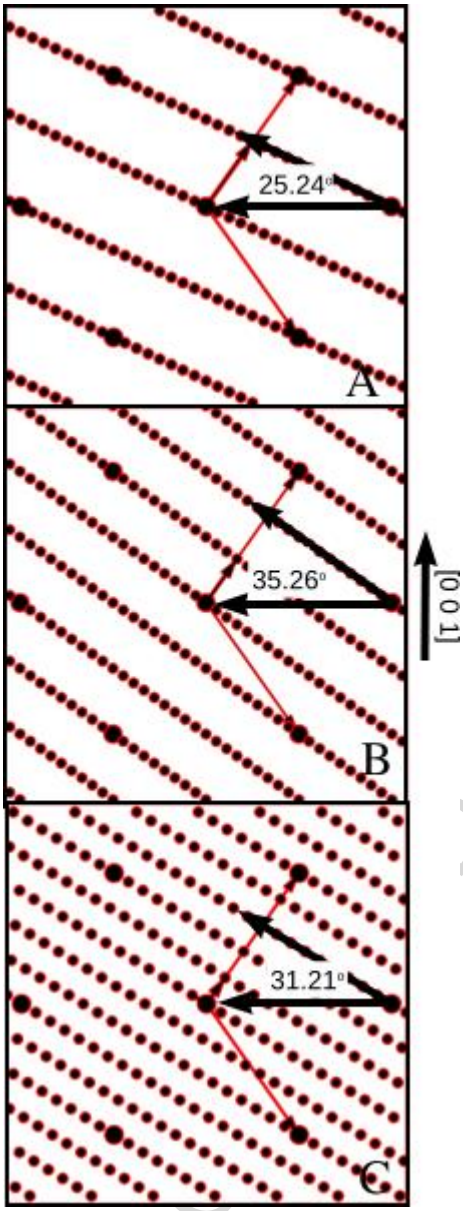

Fig. 2. Diagrams of the LEED patterns described in the text. In figure **A** the domain is along [$\bar{1}$ 1 3], **B** is along [$\bar{1}$ 1 2], and **C** is along the [$\bar{3}$ 3 7]

.

3.2 STM

In the STM imaging of this surface, figure 3a, we can see rows along the W [$\bar{3}$ 3 7] direction which are 24.5 ± 1.2 Å wide, as predicted from the LEED data. These rows appear as bright regions with dark depressions in between them, giving an apparent corrugation of 0.5 ± 0.05 Å ***with a +68 mV sample bias and 0.1 nA tunnelling current. This contrast is consistent over the applied bias range of ± 1.1 V, but the corrugation***

changes. We measured a a maximum corrugation of 0.7 ± 0.07 Å at -60 mV and a minimum of about 0.4 Å at ± 1.1 V. This image also gives us a very detailed picture of the oxide's atomic structure. First of all, if we follow the atomic structure along the dark region of the oxide row, we find a distinctive pattern that repeats every 13.0 ± 0.65 Å. This results in an overlayer unit cell of 24.5 ± 1.2 Å by 13.0 ± 0.65 Å equal to that measured by LEED. Additionally, from this image we can define the surface mesh created by the oxide lattice. The oxide lattice spacing is $\alpha = 2.7 \pm 0.14$ Å in a direction that is 2.5 ± 0.5° north of W [1 $\bar{1}$ 1] and $\beta = 2.4 \pm 0.14$ Å along W [0 0 1], giving a separation between the two $\phi = 68 \pm 0.5°$, and a lattice mesh very similar to the W(110) surface ([$\bar{1}$ 1 1] = [1 $\bar{1}$ 1] = 2.7 Å $\phi = 70.5$ °). If we take a line profile along the α direction there is a slight slope across the row, giving an overall difference in height of 0.15 ± 0.03 Å with the left side being lower, as shown by the line profile in figure 3b. In addition to the slope, there is a 0.1 nm shift, or stacking fault, of the atomic rows in the W[$\bar{3}$ 3 7] direction, always occurring at the dark region of the rows, as highlighted by black lines in figure 3a.

We would like to highlight that these rows are significantly different than that imaged by Johnson et. al.[10]. Firstly, these rows are orientated along a slightly different direction, [$\bar{3}$ 3 7], as opposed to [1 $\bar{1}$ 3] and they are around 10 Å narrower that that seen by Johnson et. al.. More importantly, in the case of Johnson et. al. the rows were made of dark depressions of oxygen atoms of 1:1 registry with the substrate, separated by bright domain walls attributed to being the exposed substrate. In our case we have bright rows separated by a dark region, more like that reported for the initial oxide layer of Mo(110) oxidized under similar conditions[27]. This result is not unexpected since the Mo and W are both bcc metals in the same group of the periodic table with almost identical lattice constants. In addition to this, both metals have bulk dioxides of the same distorted rutile, space group P21/C, crystal structure and near identical lattice parameters. For this reason, we will use the results from the oxidation of Mo(110) for the basis of our model. To help the reader a model of the WO_2 structure is shown in figure 4

For the case of oxidized Mo(110) we found a LEED pattern similar to that which we are reporting for oxidized W(110), with rows along the Mo[1 $\bar{1}$ 3] and Mo[$\bar{1}$1 3] directions, with a spot separation of ˜23 Å in the real space[27]. We equated this to be the result of a MoO_2(010) overlayer a that grows epitaxially on the Mo(110) surface with a coincidence structure described by matrix notation as, $\begin{bmatrix} 1 & 8 \\ -4 & 2 \end{bmatrix}$, giving an oxide overlayer with MoO_2[201] ∥ Mo[1$\bar{1}$ $\bar{3}$] and MoO_2[100] ∥ Mo[00$\bar{1}$]. DFT calculations suggest that the most stable configuration for the interfacial oxygen is in the 3-fold coordination [27,**?**], same as measured with XPD for O on W(110)[9]. Furthermore, DFT calculations were able to explain the bright rows seen in the STM images. It was found that regions with interfacial oxygen located at or near to the 3-fold site appeared

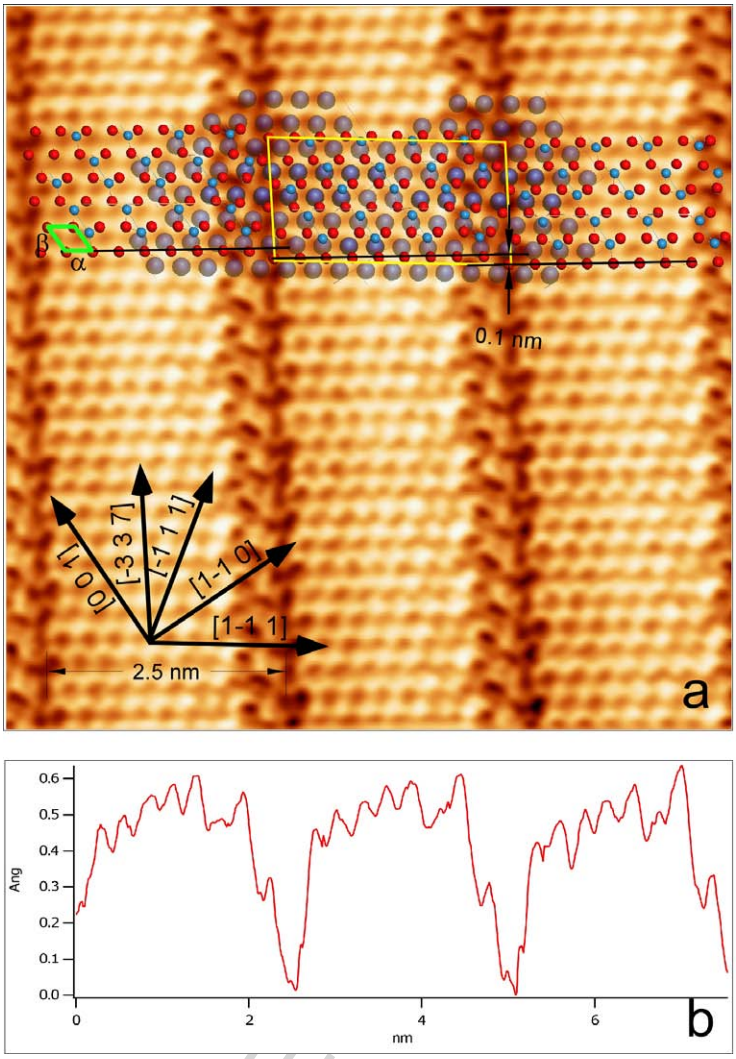

Fig. 3. a. STM image of W(110) oxidized with 1 x10^{-6} Torr oxygen at 1600 K for 60min. The image was taken at 77 K with a +68 mV sample bias and 0.1 nA tunnelling current. b. Line profile along the atomic rows in the direction marked as α, 2.5 $\pm$ 0.5° north of W [1 $\bar{1}$ 1]. ***The crystallographic directions, which were determined by LEED, are indicated in relation to W(110) and referred to in the text.***

bright, while areas located on bridge or top sites appeared dim[27]. This is a common feature of coincident lattice structures of oxides on metals[28].

Given that the rows in the STM and LEED images are the result of a coincident lattice structure between a WO_2(010) oxide layer and the W(110) surface, we can construct a model for this system. Using the atomically resolved STM image as our template, we have arranged the a WO_2(010)oxide lattice model to match the lattice imaged with STM. As shown in figure 3a, the oxygen atoms of WO_2(010) model, represented by the red circles, match with the bright spots in the STM image, which represent the atomic lattice of the real oxide surface. To achieve this we have orientated the WO_2[100]

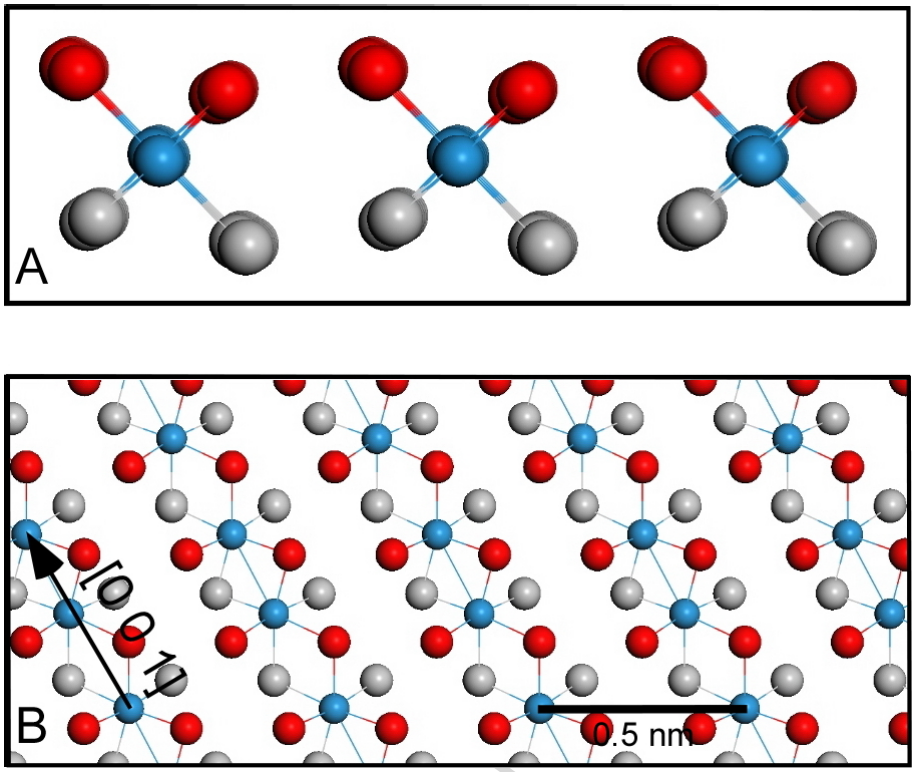

Fig. 4. A model of the WO_2 structure. Part A shows the side view of WO_2 (010) plane with the top (bottom) oxygen layer in red (grey) and the tungsten layer in blue, forming a O-M-O trilayer. Part B shows a top view of the same structure. Notice the W-W dimers that form along the [0 0 1] axis.

axis along W[00$\bar{1}$], just as with the case for the MoO_2/Mo(110) system[27]. Furthermore we needed to add a dislocation by shifting oxide lattice down 0.1 nm in the [$\bar{3}$ 3 7] direction at the left edge of each oxide row. The next step was to add the underlying W(110) surface to the model to show the relationship between the oxide layer and oxide the surface. This model, shown as the larger blue circles in 3a, is positioned such that the oxygen atoms at the corners of the superstructure unit cell (yellow box) are located above 3-fold sites of the W(110) surface. This position is known to be the most energetically favorable position for oxygen on the W(110) and Mo(110) surface. As one moves from this point to the right, along the W[1 $\bar{1}$ 1] direction the oxygen atoms are located on a two fold site, and then their position moves gradually towards the least energetically favorable (1.2 eV higher), on-top position [29]. However, after 8 units, we see that there is a shift and the 9th oxygen atom is located again on the 3-fold site. There is further evidence of this progression in the line profile of the STM image along this direction(figure 3b). This line profile shows there is a gradual slope, with the left most, three fold coordinated, oxygen atom being the lowest. As we travel down the line, and as the interface oxygen atoms are located more and more towards the on top position, we have a gradual increase in height until there is a shift and the oxygen is again located at the three fold coordinated position. One could think that this is

the ultimate result of a compromise between strain in the oxide layer and the adsorption energy of oxygen at the interface. ***Furthermore, with such a structure there is a 1:1 ratio of oxygen and tungsten incorporated in the metal surface and oxide layer. This would be in agreement with the values for the saturated oxide layer as measured by others [2,5].***

4 Conclusion

We have shown that a WO_2(010) oxide layer grows on the W(110) surface when the sample is annealed at between 1000 K to 1600 K in an oxygen environment of 1 x10^{-6}Torr oxygen pressure. Using LEED and STM we found that this oxide layer forms a row structure on the surface with a unit cell that is described in matrix notation as

$$\begin{bmatrix} 0 & 9 \\ -2 & 5 \end{bmatrix}$$

. By matching a structure model of the WO_2(010) and W(110) surface to the atomically resolved STM data we were able to construct a model for the oxide layer. ***This model is consistent with the model developed for that of the very similar MoO_2/Mo(110) system.*** While the structure of both Molybdenum and Tungsten as well as their dioxides are almost identical, we find a similar, but noticeably different coincident structures for the two systems. Considering that the interface energy between the metal and oxide is a balance between the elastic properties and the binding energy between the two, it is reasonable to expect that differences in these properties (which have been completely neglected in our geometrical description) could lead to the slight differences that we see in the two systems.

It is known that there is one further difference between tungsten and molybdenum oxides. At high pressure tungsten oxide can undergo transformation into an orthorhombic phase[30]. This is not the case for the molybdenum oxides. Such an orthorhombic oxide could conceivably be formed on the W(110) surface under the influence of lattice mismatch strain in our sample. This could open another avenue for establishing a model alternative to the one presented in the paper to explain experimental results obtained. We did not pursue this avenue due to the complexity of the orthorhombic tungsten oxide phase. Instead we favored a simpler explanation.

This work was supported by the Science Foundation Ireland (SFI), Principal Investigator Grant No 06/IN.1/I91.

References

[1] T. Engel, H. Niehus, E. Bauer, Surf. Sci. 52 (1975) 237.

[2] E. Bauer, T. Engel, Surf. Sci. 71 (1978) 695 – 718.

[3] P. K. Wu, M. C. Tringides, M. G. Lagally, Phys. Rev. B 39 (1989) 7595.

[4] M. C. Tringides, Phys. Rev. Lett. 65 (1990) 1372.

[5] R. X. Ynzunza, F. J. Palomares, E. D. Tober, Z. Wang, J. Morais, R. Denecke, H. Daimon, Y. Chen, Z. Hussain, M. A. V. Hove, C. S. Fadley, Surf. Sci. 442 (1999) 27.

[6] R. X. Ynzunza, R. Denecke, F. J. Palomares, J. Morais, E. D. Tober, Z. Wang, F. J. G. de Abajo, J. Liesegang, Z. Hussain, M. A. V. Hove, C. S. Fadley, Surf. Sci. 459 (2000) 69.

[7] D. E. Muzzall, S. Chiang, Mater. Res. Soc. Symp. Proc. 619 (2000) 57.

[8] L. Germer, J. May, Surf. Sci. 4 (1966) 452.

[9] H. Daimon, R. Ynzunza, J. Palomares, H. Takabi, C. S. Fadley, Surf. Sci. 408 (1998) 260.

[10] K. E. Johnson, R. J. Wilson, S. Chiang, Phys. Rev. Lett. 71 (1993) 1055.

[11] H. Takagi, H. Daimon, F. J. Palomares, C. S. Fadley, Surf. Sci. 470 (2001) 189.

[12] M. A. Van Hove, S. Y. Tong, Phys. Rev. Lett. 35 (1975) 1092.

[13] S. Degen, A. Krupski, M. Kralj, A. Langner, C. Becker, M. Sokolowski, K. Wandelt, Surf. Sci. 576 (2005) L57.

[14] M. W. Finnis, J. Phys. Condens. Matter 8 (1996) 5811.

[15] J. Purton, S. C. Parker, D. W. Bullett, J. Phys. Condens. Matter 9 (1997) 5709.

[16] D. J. Siegel, L. G. Hector, J. B. Adams, Phys. Rev. B 65 (2002) 085415.

[17] M. Todorova, W. X. Li, M. V. Ganduglia-Pirovano, C. Stampfl, K. Reuter, M. Scheffler, Phys. Rev. Lett. 89 (2002) 096103.

[18] J. Gustafson, A. Mikkelsen, M. Borg, E. Lundgren, L. Kohler, G. Kresse, M. Schmid, P. Varga, J. Yuhara, X. Torrelles, C. Quiros, J. N. Andersen, Phys. Rev. Lett. 92 (2004) 126102.

[19] A. Stierle, F. Renner, R. Streitel, H. Dosch, W. Drube, B. C. Cowie, Science 303 (2004) 1652.

[20] J. Gustafson, A. Mikkelsen, M. Borg, J. N. Andersen, E. Lundgren, C. Klein, W. Hofer, M. Schmid, P. Varga, L. Kohler, G. Kresse, N. Kasper, A. Stierle, H. Dosch, Phys. Rev. B 71 (2005) 115442.

[21] C. T. Campbell, Phys. Rev. Lett. 96 (2006) 066106.

[22] C. I. Carlisle, D. A. King, M.-L. Bocquet, J. Cerdá, P. Sautet, Phys. Rev. Lett. 84 (2000) 3899.

[23] E. Lundgren, G. Kresse, C. Klein, M. Borg, J. N. Andersen, M. De Santis, Y. Gauthier, C. Konvicka, M. Schmid, P. Varga, Phys. Rev. Lett. 88 (2002) 246103.

[24] W.-X. Li, C. Stampfl, M. Scheffler, Phys. Rev. Lett. 90 (2003) 256102.

[25] K. Reuter, M. Scheffler, Appl. Phys. A 78 (2004) 793.

[26] C. Dri, C. Africh, F. Esch, G. Comelli, O. Dubay, L. Kohler, F. Mittendorfer, G. Kresse, P. Dudin, M. Kiskinova, J. Chem. Phys. 125 (2006) 094701.

[27] K. Radican, N. Berdunov, G. Manai, I. V. Shvets, Phys. Rev. B 75 (2007) 155434.

[28] H. C. Galloway, P. Sautet, M. Salmeron, Phys. Rev. B 54 (1996) R11145.

[29] M. Stohr, R. Podloucky, S. Muller, J. Phys. Condens. Matter 21 (2009) 134017.

[30] M. Sundberg, P. E. Werner, I. P. Zibrov, Zeitschrift fur Kristallogr. 209 (1994) 662.